Digital Preservation of the Hirsau Abbey by Means of HDS and Low Cost Close Range Photogrammetry

Zusammenfassung:

Für die Dokumentation historischer Stätten werden unter anderem Methoden der Nahbereichsphotogrammetrie und terrestrisches Laserscanning eingesetzt. Diese Diplomarbeit behandelt die fotorealistischen 3D-Rekonstruktion eines Turms im Kloster Hirsau, mittels High Definition Surveying (HDS) und Nahbereichsphotogrammetrie unter Verwendung von Sensorendaten eines Smartphones. Mittels des in diesem Projekt verwendeten Smartphones lassen sich Geo-Taged-Daten (Kamera Position und Orientierung) aufzeichnen. Diese Daten wurden als externe Orientierungsparameter der Kamera verwendet und für die finale Bündelblockausgleichung verwendet. Aus klassisch photogrammetrisch generierten Punktwolken wie auch den LiDAR-Daten wurden 3D-Modelle erzeugt und mit einander verglichen. Dabei wurde festgestellt, dass die Größe der beiden Modelle nur um 3% voreinander abweicht. Dies verdeutlicht das Potential moderner Handys als Sensorsysteme für Nahbereichsphotogrammetrie

Abstract:

This study covers the reconstruction of a 3D photorealistic model of the Hirsau abbey, by means of High Definition Surveying (HDS) and close range photogrammetry based on sensors data (camera position and orientation) and images of a smartphone. A comparison was made between the 3D models made from the 3D point clouds generated by terrestrial LiDAR as well as classical photogrammetry. It was found that the two models differ by only about 3%. It shows the performance of the new generation open source mobile phones used as sensor systems for close range photogrammetry.

1. Introduction

The preservation and documentation of the world heritage sites has become an issue since many years. Cultural heritage sites are the testimonial of the unique culture and civilization of our ancients. Natural hazards, wars, urban growth and other factors always are the threats for destroying these heritages. Some of them will be destroyed in future; others have already been disappeared for ever, such as Arg-é Bam in Iran (the world's largest adobe structure, was built in 500 B.C., destroyed in 2003 by earthquake), Buddhas of Bamyan in Afghanistan (the largest examples of standing Buddha carvings in the world, was built in 6th century, destroyed in 2001 by Taliban) and many other heritages around the world. Some organizations and foundations like UNESCO, CyArk, etc. meet these problems. For example the CyArk project attempts to digitally preserve 500 of the most important heritage sites in 5 years by means of static LiDAR, surveying, photogrammetry, photography, etc.. (Fritsch, 2009)

This study is about digital preservation of the Hirsau abbey. Hirsau Abbey, formerly known as Hirschau Abbey, was once one of the most prominent Benedictine abbeys of Germany. It is located in the northern part of the black forest in Baden-Württemberg state in Germany. In this project, the cloister part, the gate tower of the Hunting Lodge, the winter refectory, the summer refectory and the monastery kitchen of the Hirsau abbey is digitally documented.

The documentation of the heritage sites need close range data acquisition methods, such as close range photogrammetry or terrestrial laser scanning (TLS). Objects in the heritage sites range from

small artifacts on the sculptures to buildings, and in many cases have no regular shapes. Often, the time for measurement is limited. Before, close range photogrammetry was the only method for these kinds of measurements. Today, laser scanners despite of their costs have become very popular for the digital preservation of the heritage sites (Böhler and Marbs, 2002). No other instrument can be equivalent to TLS, regarding the speed and the accuracy of its dense point cloud (Böhm et al., 2005).

In this project, first from the 3D point cloud generated by a static LiDAR (Leica HDS 3000) a 3D model was created, by manual fitting of basic geometric shapes to the different parts of the point cloud. Afterwards, the 3D model got real textures by wrapping the corresponding photos onto it.

This study also includes some investigations about usage of a smartphone as a multi-sensor system in close range photogrammetry. Nowadays many mobile phone manufacturers aim to provide their customers not only with a communication device, but also with useful software tools and additional sensors integrated in these devices. The motivation of using a smartphone in this project is its ability to collect geo-tagged data (camera position and orientation). It would be interesting to know how accurate these data are, and if they can be used as approximate values (weak datum information) of the exterior orientation parameters in a bundle block adjustment process.

In this study, after the camera calibration, the gate tower of the Hirsau Abbey was measured by our terrestrial laser scanner (as a reference), and then was photographed using the HTC Hero smartphone's camera. A comparison was finally made between the CAD models resulted from these two approaches, to show the performance of this smartphone as a multi-sensor in classical photogrammetry.

2. 3D Reconstruction by means of High Definition Surveying (HDS)

In recent years, advances in the terrestrial laser scanners manufacturing provide the world of surveying with more accurate, more reliable and faster instruments through the different techniques (e.g. time of flight, phase based, etc.) for capturing as-built information. This development has created a new era in surveying: the era of "High Definition Surveying" (HDS). (Frei et al., 2004)

In this study we used a Leica HDS 3000 terrestrial laser scanner for the data acquisition. The density of the point cloud was about 5cm, which is enough for the façades, and 1cm for the fine features like decorations and the interior part of the windows in the cloister.

The point clouds were then aligned with an accuracy of about 4mm, using the Cyclone software. Modeling in this project was done by triangulation (for terrain model) and best fitting of the basic geometric shapes (patch, sphere, cylinder, box, cone, etc.) to the different parts of the point cloud (figure 1). The point cloud was segmented manually in this project using the Cyclone software. In this project, all the features larger than 20cm size are included in modeling. The decoration details of the objects larger than 10cm are also considered to be modeled.

The generated 3D model then got photorealistic by texture mapping using the Google Sketchup software, manually. The results then were uploaded to Google Earth and CyArc project.
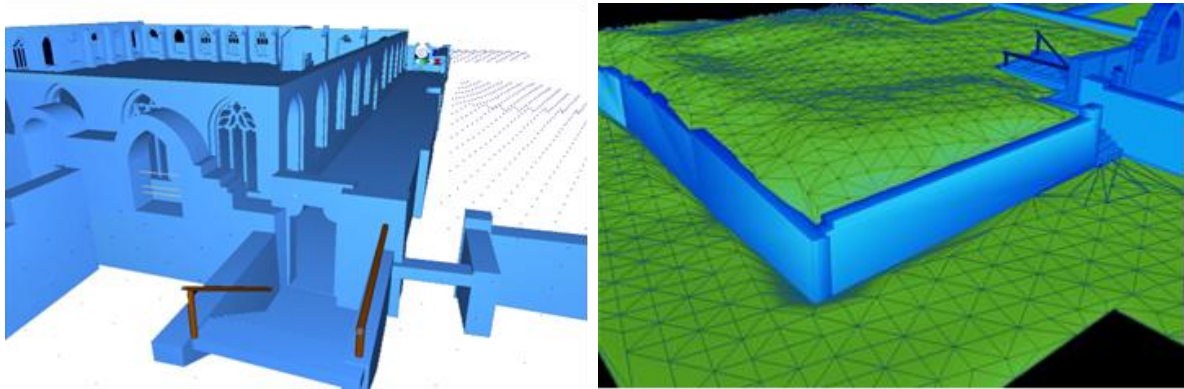
Figure 1. 3D modeling by shape fitting and triangulation

Figure 2. Integration of the 3D model in Google Earth

3. Experiences with Low Cost Close Range Photogrammetry Using a Smartphone

Smartphones are equipped with some useful sensors as well as open source operating systems to provide the user the full control of the sensors. What attracts our attention in the field of close range photogrammetry is the ability to collect geo-tagged data together with a built-in camera, which is a low accuracy and a low cost simulation of GPS/IMU supported systems.

The first step for the analysis of the sensors data is the camera calibration. The mobile phone used in this project, HTC Hero, benefits from the Google's Android open source operating system. This enabled us to write our own software for the sensors data acquisition. Then the quality of the sensors data, focused as the exterior orientation parameters, was estimated in a bundle adjustment.

3.1. Camera Calibration

The HTC Hero smartphone uses a CMOS 5 megapixels sensor for photography, which is sufficient for low to medium precision close range photogrammetric applications. For the camera calibration, a suitable 2D calibration field was used. Using a suitable image configuration, the camera was calibrated in a free net adjustment process based on the well-known Brown model (Brown, 1971) for correction of the lens distortion, using the Australis software.

The RMS of residuals was around one third of a pixel size. The main reason of such a relatively large amount of residuals might be the quality of images and the simple lens system. As far as the JPEG format is a lossy image format, the image coordinates are measured erroneous (Gruen and Akca, 2007). Also the Brown model seems not to be sufficient for the optical calibration of this low-cost camera system.
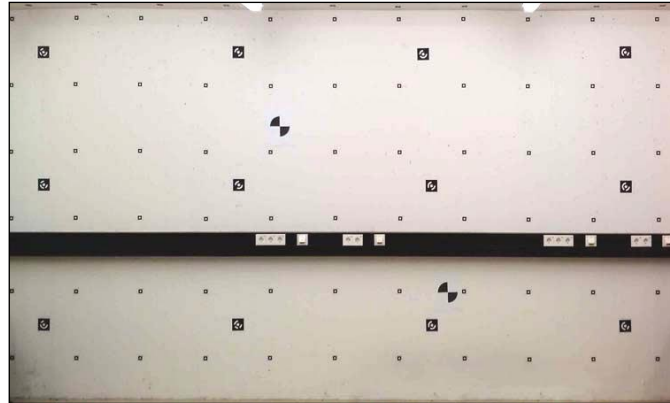

Figure 3. Calibration test field

3.2. Sensors' data Quality Assessment

The HTC Hero phone employs a 3-axis accelerometer (Bosch Sensortec BMA150), a 3-axis electronic compass (Asahi Kasei AK8973) and a GPS antenna (Le et al., 2009). The exterior orientation parameters can be derived from the output of these sensors.

Having the digital compass and the accelerometer data, the phone gives the orientation angles azimuth, and roll. The following coordinate system is adapted to this project: The X-axis is UTM easting, the Y-axis is the UTM northing and the Z-axis completes a right handed system.

3.3. Accuracy of the Integrated Sensors

GPS: The accuracy of GPS by single point positioning (navigational solution) is about 15-25 meters in open space (95% confidence level). Having redundant satellite data, the accuracy of the single point positioning can be much higher than this amount. Moreover, if a set of points is measured in a relatively short time period, as far as the satellite constellation changes slowly and all the points receive satellite signals from a same ionospheric patch, the relative positioning accuracy would be improved dramatically (Enge et al., 1988; El-Rabbany, 2002). The new generation of hand-held GPS receivers is enabled to use WAAS and EGNOS services which provide users with ionospheric corrections (Federal Aviation Administration website; European Space Agency website). It reduces therefore the main GPS error source.

Accelerometer and Digital Compass: According to (Le et al., 2009), the standard deviation given by the accelerometer sensor used by the HTC Hero is around 0.025 [m/S^2].

The standard deviation given by such a digital compass is around 0.431 μT. The magnetic field of the Earth varies from 30 μT (in SI units: $1T=1Kg/AS^2$) around the equator to approximately 60 μT near to the poles. When the device is not moving, the only acceleration is caused by gravity. Therefore one can compute the rotation angles (around 3 axes of object coordinate system) using the magnitudes of the acceleration components on the device's 3 axes and the digital compass data.

To have an idea about the standard deviations of the orientation angles given by such a device, the device was placed in a horizontal, then a vertical and finally an arbitrary position to collect the orientation data (at least 20 samples per case). Results are given in the following table.

Angle	Mode	Average	Std. Dev.
Azimuth	Horizontal	-160.0°	1.0°
Azimuth	Vertical	254.0°	8.0°
Azimuth	Arbitrary	89.6°	1.3°
Pitch	Horizontal	4.5°	0.2°
Pitch	Vertical	-87.7°	0.3°
Pitch	Arbitrary	-40.0°	0.3°
Roll	Horizontal	-0.8°	0.1°
Roll	Vertical	57.7°	7.7°
Roll	Arbitrary	0.0°	0.2°

Table 1. Empirical standard deviation of the orientation angles

Sensors Calibration: Having placed the device on a flat horizontal place, an offset of around 4.5 degrees can be seen in the pitch angle, and almost no offset in the roll angle. It can be considered in the calculations afterwards.

3.4.Sensors' Data Focused as the Exterior Orientation Parameters

To have an impression about the usage of these sensors in photogrammetric close range applications, the sensor data were contributed in a bundle block adjustment, as the initial values of the exterior orientation parameters, also called 'weak' datum. Then these initial values were compared to their estimated values.

The case of study is the gate tower close to the ruins of Hunting Lodge located at the Hirsau Abbey site. A block of 8 images forming a ring configuration was set up (Waldhaeusl and Ogleby, 1994).
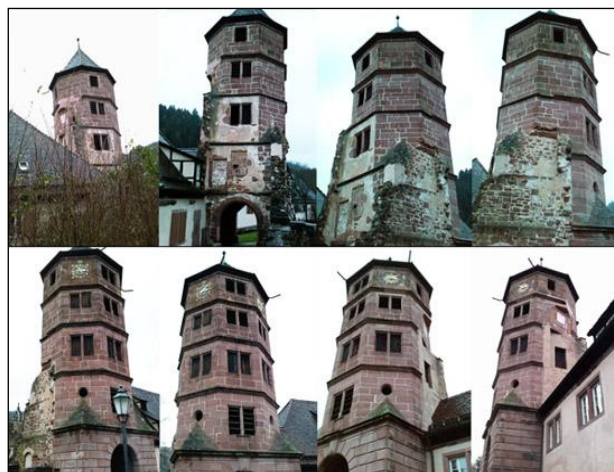

Figure 4. The gate tower of the Hirsau Abbey as the case study

The initial values of the object coordinates can be computed either by forward intersection having the sensors' data as the approximation of the exterior orientation parameters, or by relative/absolute orientation.
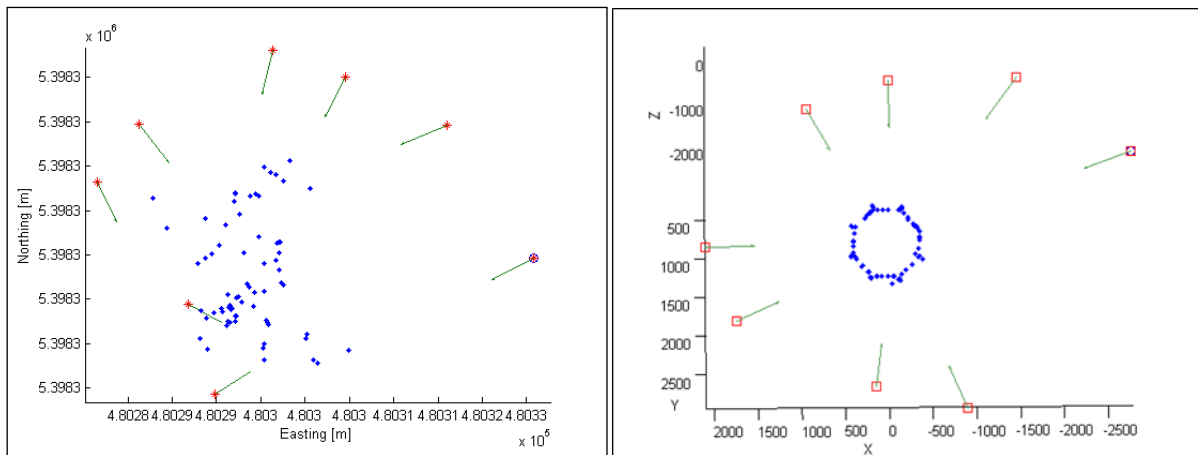
Figure 5. Forward intersection using the sensors data as exterior orientation parameters (left), Model created by relative orientation (right)

First we try the first strategy, forward intersection. Unfortunately the approximate values for the object coordinates generated by this strategy are way off for the convergence of the bundle adjustment.

From the directions of the arrows in the figure above which are the directions of photography, one may realize that the main reason of intersection errors is the errors in azimuth angles. We will verify it later. The problem of the approximate values for the object coordinates can be solved by the second strategy. The relative orientation of the photos is used for the computation of the model coordinates, and a successive absolute orientation is employed for the computation of the object coordinates (by a 3D similarity transformation). The 3D similarity transformation parameters can be calculated by comparing two sets of coordinates: UTM-coordinates of the camera projection centers (from the given GPS coordinates), and their counterparts in the model space. For getting a higher accuracy, points with higher residuals should not contribute furthermore in the analysis of the transformation parameters; since it has a direct effect on the scale of the 3D model. Moreover, if the place of photography is nearly flat, an average value can be considered for all GPS heights.

Having computed the new set of the approximate values for the object coordinates, the bundle block adjustment can be re-implemented. The bundle block adjustment is implemented in 2 scenarios:

Scenario 1: The observations of the camera position and the camera orientation are added to the system of equations (over-determined system).

Scenario 2: The bundle block adjustment is implemented using the free net adjustment (Fritsch and Schaffrin, 1981). The image coordinates are our observations only. The observations of the camera position and the camera orientation are just used as the approximate values of the unknown exterior orientation parameters.

In the first scenario, the observations of the camera positions and orientations are a part of the observations. At the same time they will receive some correction terms in the adjustment, because they are unknown parameters. Therefore there is no need to use the Gauss-Helmert model for the adjustment, as the Gauss-Markov model is sufficient for all parameter estimations. The outliers are detected and removed using the DIA test principle (Baarda, 1968). The outliers in this case are 4 azimuth angles and 4 GPS coordinates sets.

In the second scenario, the shape of the model is not influenced by possible inconsistencies between the datum observations (the camera positions and orientations). In this case the model is fitted to the initial values of the unknown parameters. The datum observations which are marked as the blunders in the first scenario, will not contribute to the datum definition in this scenario. Regarding the Helmert model for the variance components estimation (VCE) (Grafarend et al., 1980), the following standard deviations are estimated for each set of the observations:

Parameter	Std. Dev.	Estimated Std. Dev. factor
Image coordinates	1 pixel	0.4
Azimuth	6.5°	1.0
Pitch and Roll	5.2°	1.0
Easting and Northing	0.50 [m]	1.0
Height	0.36 [m]	1.0

Table 2. Estimated standard deviations for each set of the observations

The results show that we can expect an accuracy of about 5°-6° for the camera orientations and 0.3-0.5 [m] for the camera positions; however a large number of blunders exist in the observations. The reason of getting such a small standard deviation factor for the image coordinates is the magnitude of the image coordinates residuals, which are unusually small. The small residuals are not always desirable, since they might be an indication of existence of poor controlled parts in the network. The analysis of the local redundancy numbers verifies this assumption (Leick, 2004); some of the local redundancy numbers are near to zero. This can be because of imperfections in the geometry of the rays' intersection. This rather weak intersection is because of the thin shape of the object in combination with the ring configuration of the images. It can be avoided by strengthening the geometry of the network for these parts, i.e. by efficiently increasing of the number of images.
Estimated standard deviation of the unknown parameters:

Camera positions:

RMS Std. Dev.	Scenario 1	Scenario 2
Easting [m]	0.439	0.041
Northing [m]	0.439	0.040
Height [m]	0.293	0.027

Table 3. Estimated standard deviation of the camera positions

Camera orientations:

RMS Std. Dev.	Scenario 1	Scenario 2
Azimuth [deg]	1.7	0.2
Pitch [deg]	0.7	0.1
Roll [deg]	1.6	0.2

Table 4. Estimated standard deviation of the camera orientations

Object coordinates:

RMS Std. Dev.	Scenario 1	Scenario 2
Easting [m]	0.327	0.021
Northing [m]	0.326	0.021
Height [m]	0.283	0.028

Table 5. Estimated standard deviation of the object coordinate

The estimated standard deviations of the unknown parameters seem to be more realistic in scenario 1, regarding the accuracy of GPS measurements. In scenario 2, these values are only the internal accuracies, and are not influenced by the datum definitions (datum observations). They are more suitable for the analysis of the geometry of the network.

At the end of this section, a question is still remaining to be answered: if the problem of the digital compass can be solved somehow, could the forward intersection generate appropriate initial values for the object coordinates? To answer this question, the forward intersection is re-implemented using raw sensor data, but corrected azimuths, and bundle block adjustment afterwards.
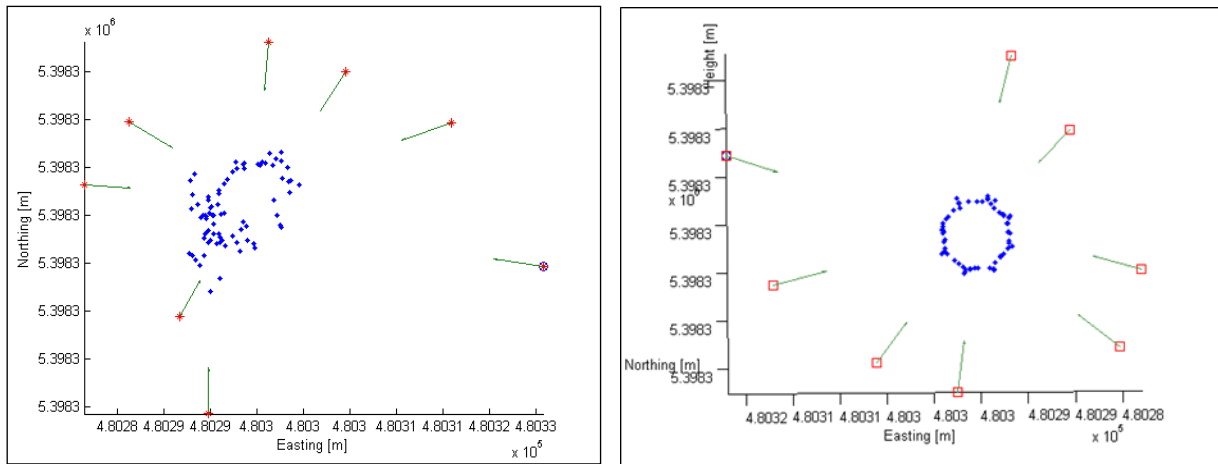

Figure 6. Forward intersection with raw sensor data but corrected azimuths (left), Results of the bundle block adjustment (right)

Fortunately in this case the bundle block adjustment has converged to 1mm after 9 iterations.

4. Verification of the 3D Model

The absolute accuracy of a photogrammetric network can be estimated by comparing the photogrammetrically determined points or distances with reference values (control data) measured independently with a higher accuracy. For this reason, some distances on the models created by close range photogrammetry are compared with the same distances on a 3D model created by terrestrial laser scanner (TLS) data as the reference. The measured distances are the widths of the façades of the modeled tower (which is an octagonal cylinder).
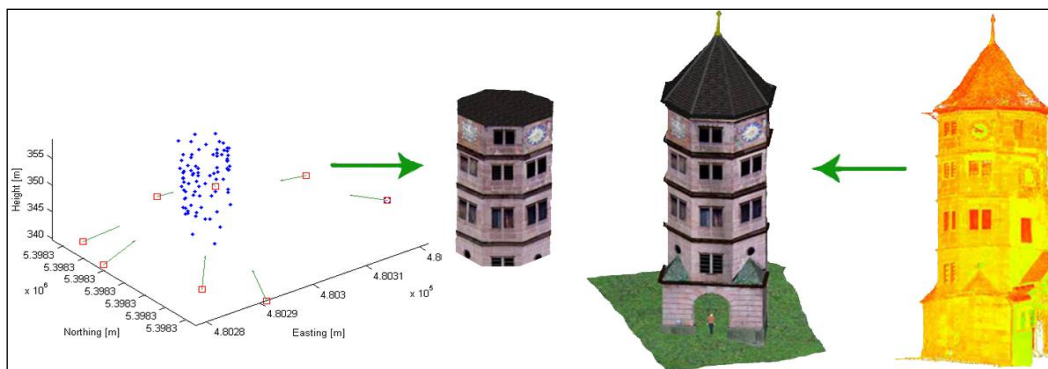

Figure 7. 3D models created by the described method (left) and terrestrial laser scanner (right)

The model created by the over-determined system (scenario 1) is around 3% smaller (96% significance) than the model created by TLS data. For the free net adjustment (scenario 2), the model is around 2% (85% significance) larger than the model created by TLS data.

	L_1[m]	L_2[m]	Scale= L_1/L_2	$L_2.\text{Scale}_{Avg}-L_1$[m]
	2.767	2.886	0.959	0.027
	2.813	2.850	0.987	-0.054
	2.845	2.984	0.953	0.044
	2.820	2.909	0.969	-0.004
	2.875	2.922	0.984	-0.046
	2.873	2.956	0.972	-0.011
	2.793	2.910	0.960	0.024
	2.864	2.980	0.961	0.021
Avg.	N/A	N/A	0.968	0.000
Std. Dev.	N/A	N/A	0.012	0.036

Table 6. Scenario 1: Measured lengths for the calculation of the scale of the model, where: L_1 is the length on the subject model and L_2 is the length on the reference model.

	L_1[m]	L_2[m]	Scale= L_1/L_2	$L_2.\text{Scale}_{Avg}-L_1$[m]
	2.956	2.886	1.024	-0.011
	2.936	2.850	1.030	-0.028
	3.036	2.984	1.017	0.009
	2.973	2.909	1.022	-0.005
	3.025	2.922	1.035	-0.044
	3.045	2.956	1.030	-0.029
	2.916	2.910	1.002	0.053
	2.984	2.980	1.001	0.057
Avg.	N/A	N/A	1.020	0.006
Std. Dev.	N/A	N/A	0.013	0.037

Table 7. Scenario 2: Measured lengths for the calculation of the scale of the model, where: L_1 is the length on the subject model and L_2 is the length on the reference model.

5. Conclusions

In this study, the potential of using the new generation of smartphones as a multi-sensor system was investigated in a low cost close range photogrammetric application.

The performance of this smartphone HTC Hero was shown by a comparison between the terrestrial laser scanner's data output and the 3D point cloud generated by photogrammetric bundle block adjustment.

The accuracy bounds of the integrated sensors were safe enough for the convergence of the bundle block adjustment, except the digital compass, when it is influenced by environmental magnetic fields. A solution can be implementing the relative/absolute orientation of the photos to generate approximate values of the object coordinates.

The sensors' data (datum observations) either can be used as the initial values of the exterior orientation parameters in a free net adjustment, or can be added to the system of equations to form an over determined system. The results show a scale difference of about 2-3% in the models created by the bundle block adjustment, which can be a satisfactory result for low to medium accuracy projects.

6. Acknowledgements

I gratefully acknowledge the valuable supervision of Prof. Dr. ing. Dieter Fritsch and co-supervision of Dr. Ing. Jan Boehm and Dipl. Ing. Michael Peter on my master's thesis.

7. References

Baarda, W. (1968). A Testing Procedure for Use in Geodetic Networks, *Netherlands Geodetic Commission, Publications on Geodesy* – New Series. Vol. 2. No. 5.

Böhler, W., Marbs, A., 2002, "3D Scanning Instruments", *ISPRS/CIPA workshop on scanning for cultural heritage recording,* Corfu, Greece.

Böhm, J., Haala, N., Alshawabkeh, Y., 2005, "Automation in Laser Scanning for Cultural Heritage Applications", *International Workshop on Recording, Modeling and Visualization of Cultural Heritage. 22 - 27 May, Ascona, Switzerland.*

Brown D. C., 1971. Close Range Camera Calibration, *Photogrammetric Engineering*, Vol. 37, No. 8, pp. 855-866.

El- Rabbany, A., 2002. Introduction to GPS: the Global Positioning System, *Artech House Mobile Communication Series*, Artech House Inc.

Enge, P. K., Kalafus, R. M., Raune, M. F., 1988. Differential Operation of the Global Positioning System, *IEEE Communications Magazine*, Vol. 26, No. 7.

Frei, E., Kung, J., Bukowski, R., 2004, "High-Definition Surveying (HDS): A New Era in Reality Capture", *Proceedings of ISPRS Workshop Laser-Scanners for Forest and Landscape Assessment Freiburg, Germany, pp. 262-271.*

Fritsch, D., Schaffrin, B., 1981. The Choice of Norm Problem for the Free Net Adjustment with Orientation Parameters, *Bolletino Geodesia Science Affini*, Vol. 41, pp. 259-282.

Fritsch, D., 2009, "Preface", *Photogrammetric Week 2009 (Ed. Fritsch, D.), Wichmann Verlag, Heidelberg.*

Grafarend, E., Kleusberg, A., Schaffrin, B., 1980. An Introduction to the Variance and Covariance Component Estimation of Helmert Type, *Zeitschrift für Vermessung*, Vol. 105, No. 4., pp. 161-180.

Gruen, A., Akca, D., 2007. Mobile Photogrammetry, *Dreiländertagung SGPBF, DGPF und OVG*, Muttenz, Switzerland, 19-21 June, DGPF Tagungsband 16 / 2007, pp. 441-451.

Le, M. H. V., Saragas, D., Webb, N., 2009. Indoor Navigation System for Handheld Devices, In partial fulfillment of the requirements of the Degree of Bachelor of Science, Worcester Polytechnic Institute Worcester, Massachusetts, USA.

Waldhaeusl, P., Ogleby, C., 1994. 3x3 Rules for Simple Photogrammetric Documentation of Architecture, *ISPRS*, Vol. XXX, Part5, pp. 426-429.

Leick, A., 2004. GPS satellite surveying, 3rd edition, John Wiley & Sons Inc., New York.

European Space Agency, 2010. EGNOS for Professionals, available at:
http://www.egnos-pro.esa.int/index.html (accessed Mar. 2010)

Federal Aviation Administration, 2010. Navigation Services - WAAS - How It Works, available at:
http://www.faa.gov/about/office_org/headquarters_offices/ato/service_units/techops/navservices/gnss/waas/howitworks/ (accessed Mar. 2010)